

DIS2019

Production of $W^+ W^-$ and $t\bar{t}$ pairs via photon-photon processes in proton-proton collisions

Antoni Szczurek ^{1,2},
Marta Łuszczak ², Wolfgang Schäfer ¹, Laurent Forthomme ³

¹Institute of Nuclear Physics PAN Kraków
²University of Rzeszów

Torino, April 8-12, 2019

Introduction

- ▶ Electroweak corrections are important for precise calculations of cross sections in different processes.
- ▶ Photon distributions become topical in last years.
Mostly collinear approach was discussed.
- ▶ $\gamma\gamma \rightarrow l^+l^-$ was measured by ATLAS and CMS
- ▶ $\gamma\gamma \rightarrow W^+W^-$ testing physics beyond Standard Model
anomalous boson couplings.
Pierzchala, Piotrzkowski and Chapon, Royon and Kepka
- ▶ $\gamma\gamma \rightarrow W^+W^-$ important contribution to large M_{WW}
(M. Łuszczak, A. Szczurek, Ch. Royon).
- ▶ $\gamma\gamma \rightarrow W^+W^-$ can be separated by imposing rapidity gap condition (ATLAS and CMS).

Dilepton production

- ▶ G.G. da Silveira, L. Forthomme, K. Piotrzkowski, W. Schäfer and A. Szczurek,
"Central $\mu^+ \mu^-$ production via photon-photon fusion in proton-proton collisions with proton dissociation", JHEP **02** (2015) 159.
- ▶ M. Łuszczak, W. Schäfer and A. Szczurek,
"Two-photon dilepton production in proton-proton collisions: Two alternative approaches", Phys. Rev. **D93** (2016) 074018.
- ▶ P. Lebiedowicz and A. Szczurek,
"Exclusive and semiexclusive production of $\mu^+ \mu^-$ pairs with Delta isobars and other resonances in the final state and the size of absorption effects", Phys. Rev. **D98** (2018) 053007.

Presented here papers

- ▶ M. Łuszczak, W. Schäfer and A. Szczurek,
“Production of $W^+ W^-$ pairs via $\gamma^* \gamma^* \rightarrow W^+ W^-$ subprocess
with photon transverse momenta”, JHEP**05** (2018) 064.
- ▶ L. Forthomme, M. Łuszczak, W. Schäfer and A. Szczurek,
“Rapidity gap survival factors caused by remnant fragmentation
for $W^+ W^-$ pair production via $\gamma^* \gamma^* \rightarrow W^+ W^-$ subprocess with
photon transverse momenta”, Phys. Lett. **B789** (2019) 300.
- ▶ M. Łuszczak, L. Forthomme, W. Schäfer and A. Szczurek.
“Production of $t\bar{t}$ pairs via $\gamma\gamma$ fusion with photon transverse
momenta and proton dissociation”, JHEP**02** (2019) 100.

Formalism

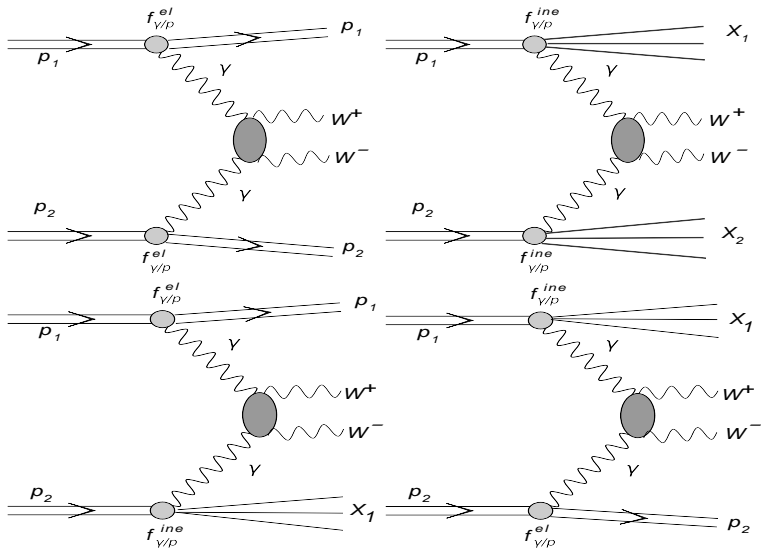
Master formula:

$$\frac{d\sigma^{(i,j)}}{dy_1 dy_2 d^2 \mathbf{p}_1 d^2 \mathbf{p}_2} = \int \frac{d^2 \mathbf{q}_1}{\pi q_1^2} \frac{d^2 \mathbf{q}_2}{\pi q_2^2} \mathcal{F}_{\gamma^*/A}^{(i)}(x_1, \mathbf{q}_1) \mathcal{F}_{\gamma^*/B}^{(j)}(x_2, \mathbf{q}_2) \frac{d\sigma^*(p_1, p_2; \mathbf{q}_1, \mathbf{q}_2)}{dy_1 dy_2 d^2 \mathbf{p}_1 d^2 \mathbf{p}_2}, \quad (1)$$

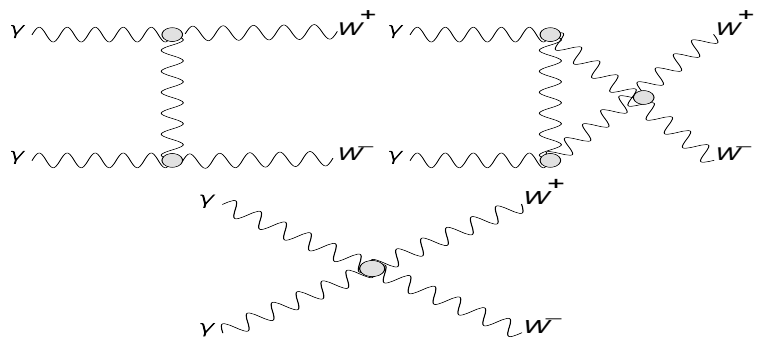
As for k_t -factorization approach in gluon-gluon induced processes
i,j = elastic, inelastic

$$\begin{aligned} x_1 &= \sqrt{\frac{\mathbf{p}_1^2 + m_W^2}{s}} e^{y_1} + \sqrt{\frac{\mathbf{p}_2^2 + m_W^2}{s}} e^{y_2}, \\ x_2 &= \sqrt{\frac{\mathbf{p}_1^2 + m_W^2}{s}} e^{-y_1} + \sqrt{\frac{\mathbf{p}_2^2 + m_W^2}{s}} e^{-y_2}. \end{aligned} \quad (2)$$

Mechanisms discussed in the presentation



Elementary process, diagrams



t-,u- and contact diagrams

Matrix elements

Elementary off-shell cross section:

$$\frac{d\sigma^*(p_1, p_2; \mathbf{q}_1, \mathbf{q}_2)}{dy_1 dy_2 d^2\mathbf{p}_1 d^2\mathbf{p}_2} = \frac{1}{16\pi^2(x_1 x_2 s)^2} \sum_{\lambda_{W^+} \lambda_{W^-}} |M(\lambda_{W^+}, \lambda_{W^-})|^2 \delta^{(2)}(\mathbf{p}_1 + \mathbf{p}_2 - \mathbf{q}_1 - \mathbf{q}_2), \quad (3)$$

Helicity-dependent off-shell matrix elements

$$\begin{aligned} M(\lambda_{W^+}, \lambda_{W^-}) &= \frac{1}{|\vec{q}_{\perp 1}| |\vec{q}_{\perp 2}|} \sum_{\lambda_1 \lambda_2} (\vec{e}_{\perp}(\lambda_1) \cdot \vec{q}_{\perp 1})(\vec{e}_{\perp}^*(\lambda_2) \cdot \vec{q}_{\perp 2}) \mathcal{M}(\lambda_1, \lambda_2; \lambda_{W^+}, \lambda_{W^-}) \\ &= \frac{1}{|\vec{q}_{\perp 1}| |\vec{q}_{\perp 2}|} \sum_{\lambda_1 \lambda_2} q_{\perp 1}^j q_{\perp 2}^j e_i(\lambda_1) e_j^*(\lambda_2) \cdot \mathcal{M}(\lambda_1, \lambda_2; \lambda_{W^+}, \lambda_{W^-}), \end{aligned} \quad (4)$$

Initial and final state helicity-dependent matrix elements were discussed in:

O. Nachtmann, F. Nagel, M. Pospischil and A. Utermann,
Eur. Phys. J. C 45, 679 (2006)

Matrix elements

Auxiliary formula:

$$\begin{aligned} q_{\perp 1}^i q_{\perp 2}^j &= \frac{1}{2} \delta_{ij} (\vec{q}_{\perp 1} \cdot \vec{q}_{\perp 2}) + \frac{1}{2} (q_{\perp 1}^i q_{\perp 2}^j + q_{\perp 1}^j q_{\perp 2}^i - \delta_{ij} (\vec{q}_{\perp 1} \cdot \vec{q}_{\perp 2})) + \frac{1}{2} (q_{\perp 1}^i q_{\perp 2}^j - q_{\perp 1}^j q_{\perp 2}^i) \\ &= \frac{1}{2} \delta_{ij} (\vec{q}_{\perp 1} \cdot \vec{q}_{\perp 2}) + \frac{1}{2} t_{ij}^{kl} q_{\perp 1}^k q_{\perp 2}^l + \frac{1}{2} \epsilon_{ij} [\vec{q}_{\perp 1}, \vec{q}_{\perp 2}]. \end{aligned} \quad (5)$$

Helicity dependent matrix element:

$$\begin{aligned} M(\lambda_{W+} \lambda_{W-}) &= \frac{1}{|\vec{q}_{\perp 1}| |\vec{q}_{\perp 2}|} \left\{ (\vec{q}_{\perp 1} \cdot \vec{q}_{\perp 2}) \cdot (\mathcal{M}(++; \lambda_{W+} \lambda_{W-}) + \mathcal{M}(--; \lambda_{W+} \lambda_{W-})) \right. \\ &\quad - i[\vec{q}_{\perp 1}, \vec{q}_{\perp 2}] (\mathcal{M}(++; \lambda_{W+} \lambda_{W-}) - \mathcal{M}(--; \lambda_{W+} \lambda_{W-})) \\ &\quad - (q_{\perp 1}^x q_{\perp 2}^x - q_{\perp 1}^y q_{\perp 2}^y) (\mathcal{M}(+-; \lambda_{W+} \lambda_{W-}) + \mathcal{M}(-+; \lambda_{W+} \lambda_{W-})) \\ &\quad \left. - i(q_{\perp 1}^x q_{\perp 2}^y + q_{\perp 1}^y q_{\perp 2}^x) (\mathcal{M}(+-; \lambda_{W+} \lambda_{W-}) - \mathcal{M}(-+; \lambda_{W+} \lambda_{W-})) \right\}. \end{aligned} \quad (6)$$

Photons fluxes

$$dn^{\text{in,el}} = \frac{dz}{z} \frac{d^2\mathbf{q}}{\pi \mathbf{q}^2} \mathcal{F}_{\gamma^* \leftarrow A}^{\text{in,el}}(z, \mathbf{q}). \quad (7)$$

$$Q^2 = \frac{\mathbf{q}^2 + z(M_X^2 - m_p^2) + z^2 m_p^2}{(1-z)}, \quad (8)$$

$$\frac{dQ^2}{Q^2} = \frac{Q^2 - Q_{\min}^2}{Q^2} \frac{d^2\mathbf{q}}{\pi \mathbf{q}^2}, \text{ and } \frac{\mathbf{q}^2}{\mathbf{q}^2 + z(M_X^2 - m_p^2) + z^2 m_p^2} = \frac{Q^2 - Q_{\min}^2}{Q^2}, \quad (9)$$

Photon fluxes

Inelastic flux:

$$\begin{aligned}\mathcal{F}_{\gamma^* \leftarrow A}^{\text{in}}(z, \mathbf{q}) &= \frac{\alpha_{\text{em}}}{\pi} \left\{ (1-z) \left(\frac{\mathbf{q}^2}{\mathbf{q}^2 + z(M_X^2 - m_p^2) + z^2 m_p^2} \right)^2 \frac{F_2(x_{\text{Bj}}, Q^2)}{Q^2 + M_X^2 - m_p^2} \right. \\ &\quad \left. + \frac{z^2}{4x_{\text{Bj}}^2} \frac{\mathbf{q}^2}{\mathbf{q}^2 + z(M_X^2 - m_p^2) + z^2 m_p^2} \frac{2x_{\text{Bj}} F_1(x_{\text{Bj}}, Q^2)}{Q^2 + M_X^2 - m_p^2} \right\},\end{aligned}\tag{10}$$

Ingredients: F_1 and F_2 structure functions

Elastic flux:

$$\begin{aligned}\mathcal{F}_{\gamma^* \leftarrow A}^{\text{el}}(z, \mathbf{q}) &= \frac{\alpha_{\text{em}}}{\pi} \left\{ (1-z) \left(\frac{\mathbf{q}^2}{\mathbf{q}^2 + z(M_X^2 - m_p^2) + z^2 m_p^2} \right)^2 \frac{4m_p^2 G_E^2(Q^2) + Q^2 G_M^2(Q^2)}{4m_p^2 + Q^2} \right. \\ &\quad \left. + \frac{z^2}{4} \frac{\mathbf{q}^2}{\mathbf{q}^2 + z(M_X^2 - m_p^2) + z^2 m_p^2} G_M^2(Q^2) \right\}.\end{aligned}\tag{11}$$

Ingredients: Electromagnetic form factors

V. M. Budnev, I. F. Ginzburg, G. V. Meledin and V. G. Serbo,
Phys. Rept. 15, 181 (1975).

Collinear-factorization approach

$$\frac{d\sigma^{(i,j)}}{dy_1 dy_2 d^2 p_T} = \frac{1}{16\pi^2(x_1 x_2 s)^2} \sum_{i,j} x_1 \gamma^{(i)}(x_1, \mu^2) x_2 \gamma^{(j)}(x_2, \mu^2) \overline{|\mathcal{M}_{\gamma\gamma \rightarrow W^+W^-}|^2}. \quad (12)$$

Longitudinal momentum fractions:

$$\begin{aligned} x_1 &= \sqrt{\frac{p_T^2 + m_W^2}{s}} \left(\exp(y_1) + \exp(y_2) \right), \\ x_2 &= \sqrt{\frac{p_T^2 + m_W^2}{s}} \left(\exp(-y_1) + \exp(-y_2) \right). \end{aligned} \quad (13)$$

Parametrizations of structure functions of proton

ALLM parametrization

- ▶ H. Abramowicz, E. M. Levin, A. Levy and U. Maor Phys. Lett. **B269**, (1991) 465

$$F_2(x, Q^2) = \frac{Q^2}{Q^2 + m_0^2} \left(F_2^{\mathcal{P}}(x, Q^2) + F_2^{\mathcal{R}}(x, Q^2) \right)$$

FFJLM parametrization

- ▶ R. Fiore, A. Flachi, L. L. Jenkovszky, A. I. Lengyel and V. K. Magas - Phys. Rev. **D70**, 054003 (2004)

$$\mathcal{I}m\alpha(s) = s^\delta \sum_n c_n \left(\frac{s - s_n}{s} \right)^{\mathcal{R}e\alpha(s_n)} \cdot \theta(s - s_n)$$

$$\mathcal{R}e\alpha(s) = \alpha(0) + \frac{s}{\pi} PV \int_0^\infty ds' \frac{\mathcal{I}m\alpha(s')}{s'(s' - s)}$$

Parametrizations of structure functions of proton

SU parametrization

- ▶ A. Szczerba, V. Uleshchenko
Eur. Phys. J. **C12** (200) 663-671

$$F_2^N(x, Q^2) = F_2^{N,VDM}(x, Q^2) + F_2^{N,part}(x, Q^2)$$

$$F_2^{N,VDM}(x, Q^2) = \frac{Q^2}{\pi} \sum_V \frac{M_V^4 \cdot \sigma_{VN}^{tot}(s^{1/2})}{\gamma_V^2(Q^2 + M_V^2)^2} \cdot \Omega_V(x, Q^2)$$

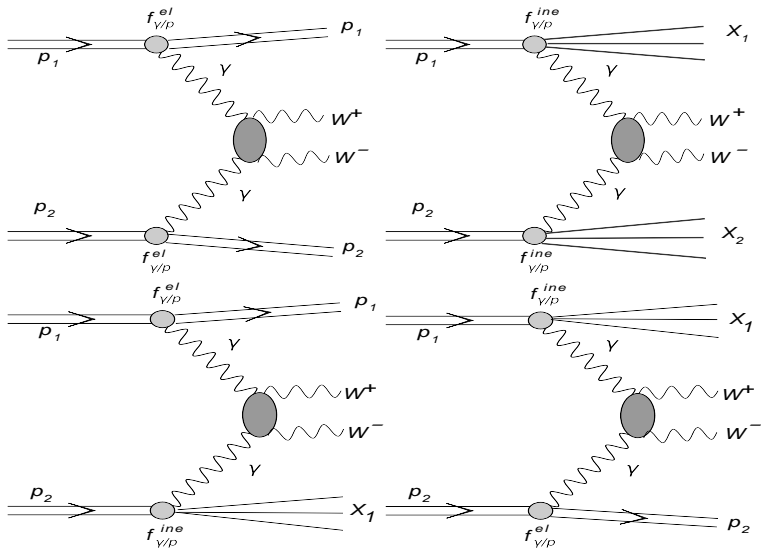
$$F_2^{N,part}(x, Q^2) = \frac{Q^2}{Q^2 + Q_0^2} \cdot F_2^{asymp}(\bar{x}, \bar{Q}^2)$$

LUX-like structure function

Recently LUX QED parametrization was proposed.

- ▶ a newly constructed parametrization, which at $Q^2 > 9 \text{ GeV}^2$ uses an NNLO calculation of F_2 and F_L from [NNLO MSTW 2008](#) partons. It employs a useful code by the MSTW group to calculate structure functions. At $Q^2 > 9 \text{ GeV}^2$ this fit uses the parametrization of [Bosted and Christy](#) in the resonance region, and a version of the ALLM fit published by the [HERMES Collaboration](#) for the continuum region. It also uses information on the longitudinal structure function from SLAC. As the fit is constructed closely following [LUX QED work](#) we call this fit [LUX-like](#).

Mechanisms discussed in the presentation

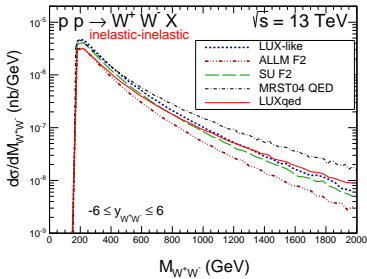
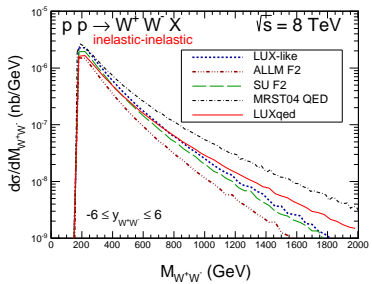


Results, integrated cross sections

contribution	8 TeV	13 TeV
LUX-like		
$\gamma_{el}\gamma_{in}$	0.214	0.409
$\gamma_{in}\gamma_{el}$	0.214	0.409
$\gamma_{in}\gamma_{in}$	0.478	1.090
ALLM97 F2		
$\gamma_{el}\gamma_{in}$	0.197	0.318
$\gamma_{in}\gamma_{el}$	0.197	0.318
$\gamma_{in}\gamma_{in}$	0.289	0.701
SU F2		
$\gamma_{el}\gamma_{in}$	0.192	0.420
$\gamma_{in}\gamma_{el}$	0.192	0.420
$\gamma_{in}\gamma_{in}$	0.396	0.927
LUXqed collinear		
$\gamma_{in+el}\gamma_{in+el}$	0.366	0.778
MRST04 QED collinear		
$\gamma_{el}\gamma_{in}$	0.171	0.341
$\gamma_{in}\gamma_{el}$	0.171	0.341
$\gamma_{in}\gamma_{in}$	0.548	0.980
Elastic- Elastic		
$\gamma_{el}\gamma_{el}$ (Budnev)	0.130	0.273
$\gamma_{el}\gamma_{el}$ (DZ)	0.124	0.267

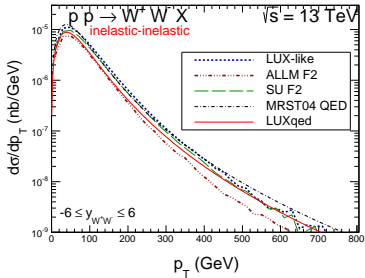
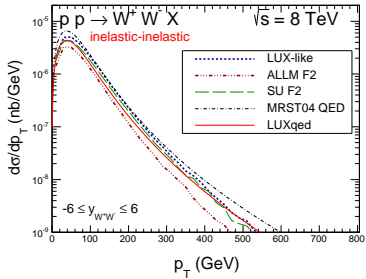
Table: Cross sections (in pb) for different contributions and different F2 structure functions: LUX, ALLM97 and SU, compared to the relevant collinear distributions with MRST04 QED and LUXqed distributions.

Results, inelastic-inelastic contribution

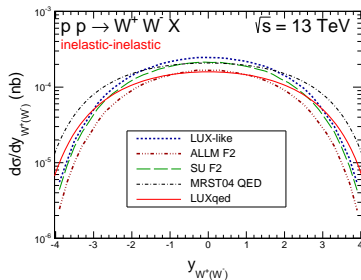
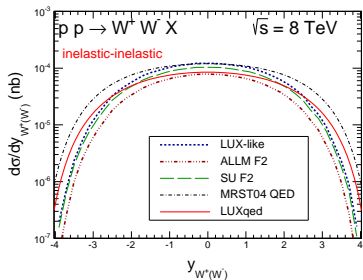


k_t -factorization result similar to the collinear
(for the same structure function (LUX-like))
old MRST04-QED collinear approach predicted larger cross section.

Results, inelastic-inelastic contribution

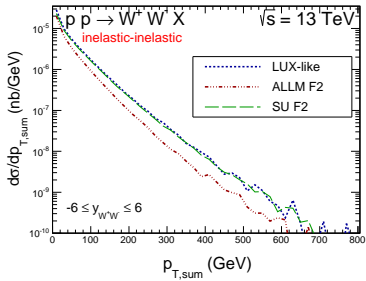
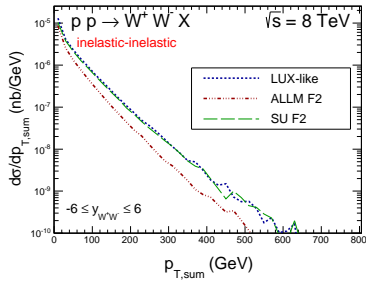


Results, inelastic-inelastic contribution



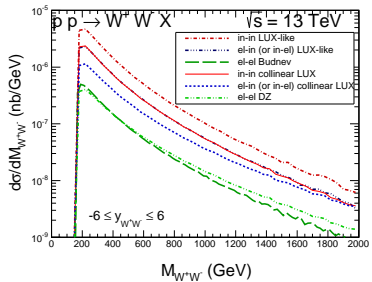
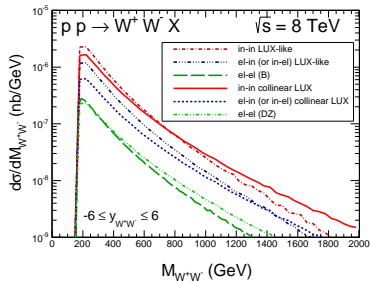
Similar results at midrapidities

Results, inelastic-inelastic contribution

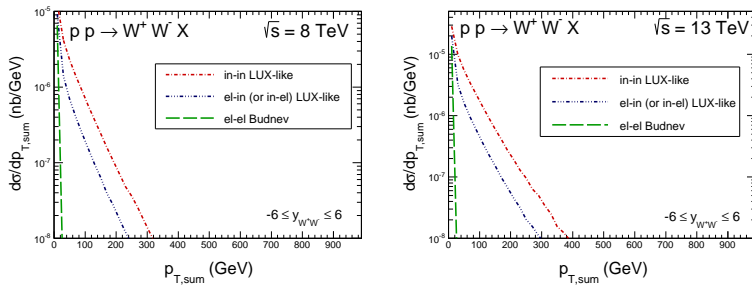


Delta function for collinear approach
But difficult to measure !

Results, different components

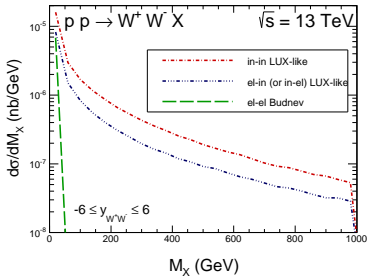
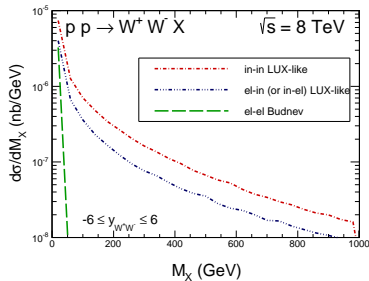


Results, different components



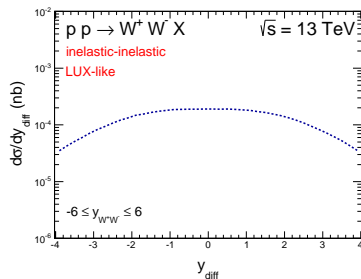
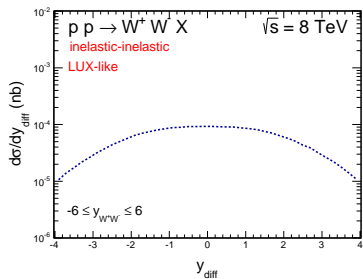
In collinear approach all of them are Dirac delta functions

Results, different components



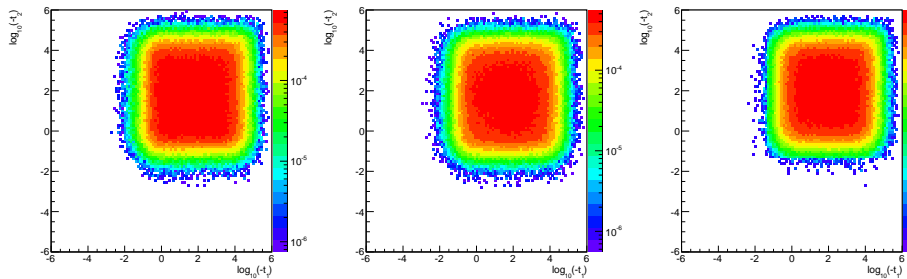
LUX-like structure functions

Results, rapidity distance between W bosons



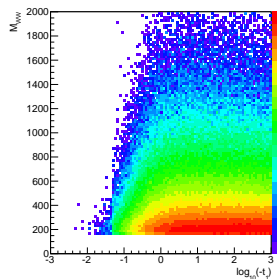
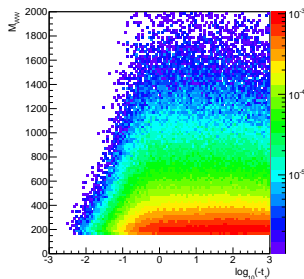
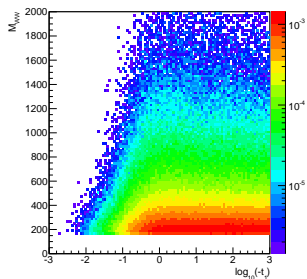
Very broad distribution, spin-1 exchange

Results, correlation variables



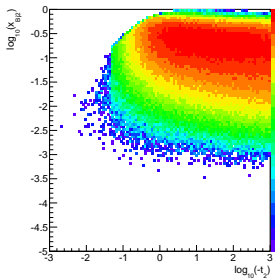
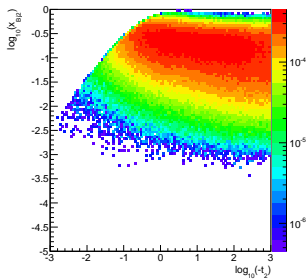
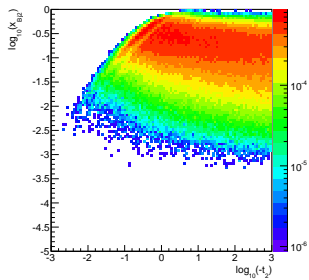
Large virtualities of photons, contradicts collinear approach
Similar pattern for different parametrizations of structure functions

Results, correlation variables

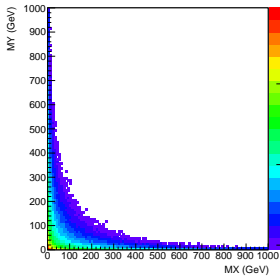
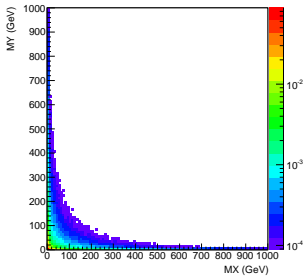
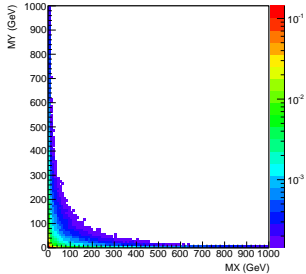


Large M_{WW} large $|t_1|$ or $|t_2|$ - strongly virtual photons

Results, correlation variables

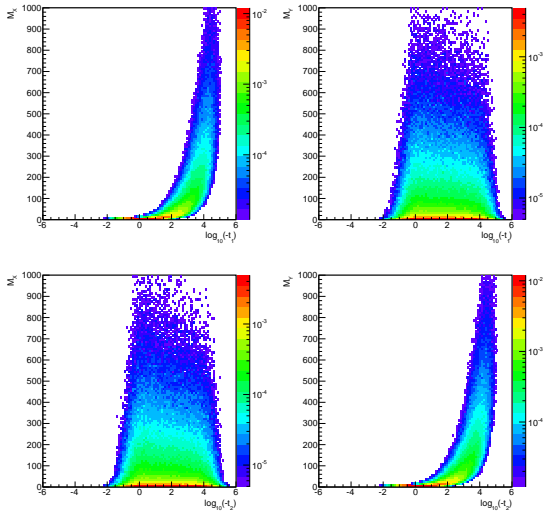


Results, correlation variables



There seem to be a correlation between M_X and M_Y
When one is large, the second seems rather small
needs more attention.

Results, correlation variables



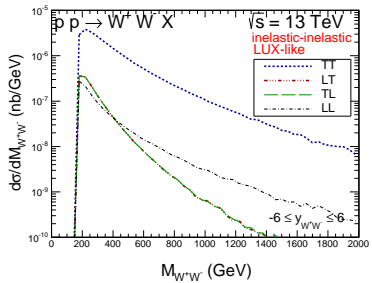
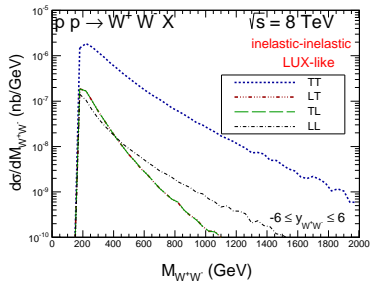
For $\sqrt{s} = 13$ TeV similar pattern

Results, spin decompositions

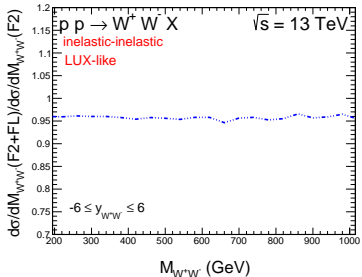
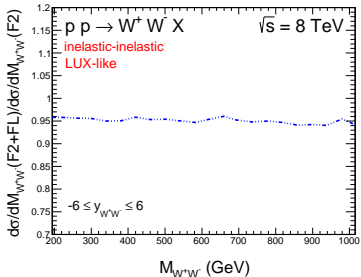
contribution	8 TeV	13 TeV
TT	0.405	0.950
LL	0.017	0.046
LT + TL	$0.028 + 0.028$	$0.052 + 0.052$
SUM	0.478	1.090

Table: Contributions of different polarizations of W bosons for the inelastic-inelastic component for the LUX-like structure function. The cross sections are given in pb .

Results, spin decompositions

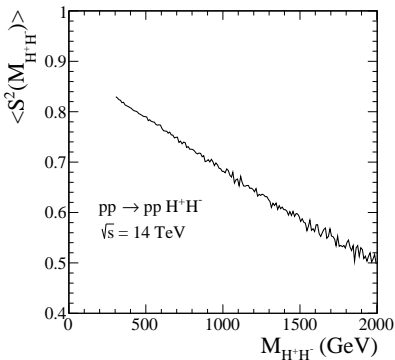


Results, longitudinal structure function



Small effect, decreasing the cross section

Gap survival for purely exclusive process



$pp \rightarrow pp H^+ H^-$

P. Lebiedowicz and A. Szcurek,

Phys. Rev. D91 (2015) 095008.

similar studies: Dynadal, Schoeffel and Harland-Lang, Khoze,
Ryskin

No dependence on rapidity gap size !!!

Gap survival related to (mini)jet emissions

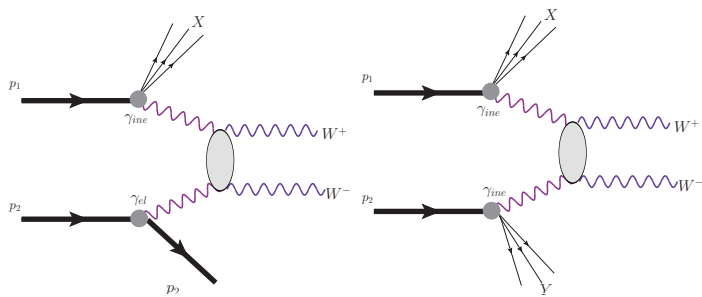


Figure: The single and double dissociative mechanisms.

The remnant fragmentation with PYTHIA 8

Including only parton emission is already quite good.

(see also Harland-Lang, Khoze, Ryskin)

General consideration

It was shown ([Luszczak et al.](#)) that without any gap survival effects:

$$\sigma(\text{inel.-inel.}) > \sigma(\text{inel.-el.}) + \sigma(\text{el.-inel.}) > \sigma(\text{el.-el.}) . \quad (14)$$

Can this ordering be changed when the rapidity gap requirement is taken into account?

$$S_R(\eta_{\text{cut}}) = 1 - \frac{1}{\sigma} \int_{-\eta_{\text{cut}}}^{\eta_{\text{cut}}} \frac{d\sigma}{d\eta_{\text{jet}}} d\eta_{\text{jet}}, \quad (15)$$

Distribution of the extra jet

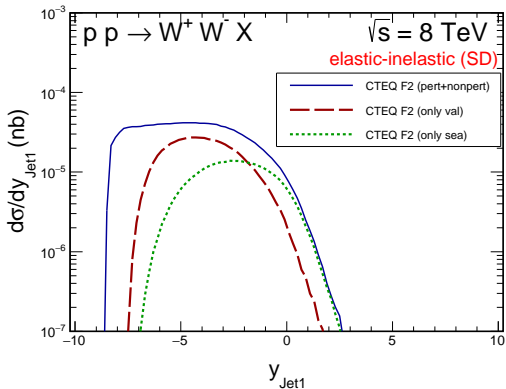


Figure: Jet rapidity distribution for F_2 using a LO partonic distribution at large Q^2 . The solid line is a sum of all contributions. The dashed line is for the valence component and the dotted line is for the sea component.

Gap survival factor associated with jet emission

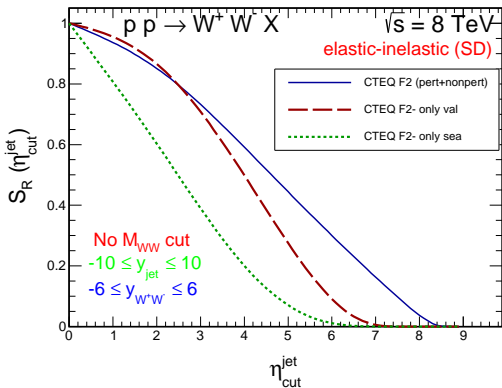


Figure: Gap survival factor associated with the jet emission and defined by Eq. (15). The solid line is for the full model, the dashed line for the valence contribution and the dotted line for the sea contribution.

Particles in the jet

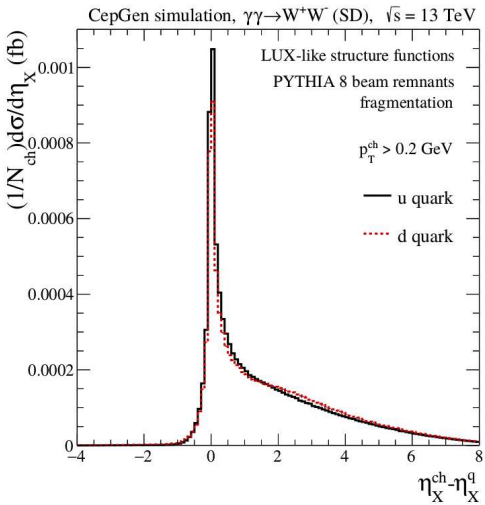
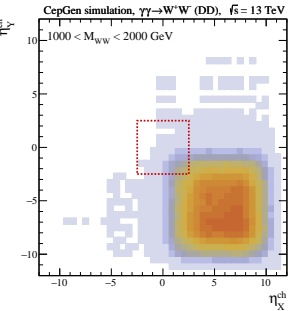
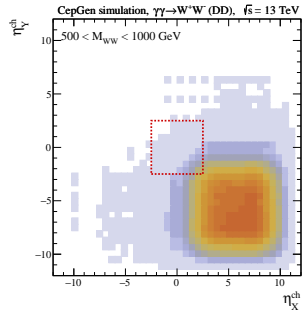
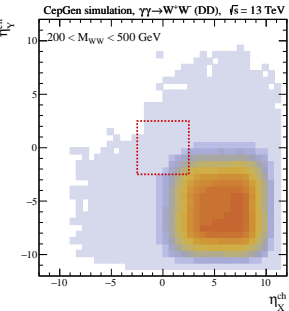
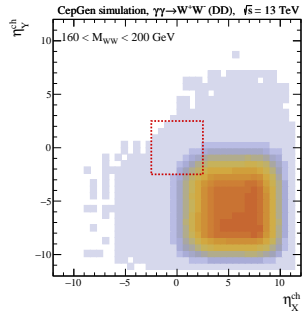


Figure: Distribution of charged particles in the single dissociative case for u (black solid line) and d (red dotted line) quarks at 13 with respect to η_{jet} .

Double dissociation



Gap survival factors for SD and DD processes

2*Contribution	$S_{R,SD}(\eta^{\text{ch}} < 2.5)$		$(S_{R,SD})^2 (\eta^{\text{ch}} < 2.5)$		$S_{R,DD}(\eta^{\text{ch}} < 2.5)$	
	8	13	8	13	8	13
(2 M_{WW} , 200)	0.763(2)	0.769(2)	0.582(4)	0.591(4)	0.586(1)	0.601(2)
(200, 500)	0.787(1)	0.799(1)	0.619(2)	0.638(2)	0.629(1)	0.649(1)
(500, 1000)	0.812(2)	0.831(2)	0.659(3)	0.691(3)	0.673(2)	0.705(2)
(1000, 2000)	0.838(7)	0.873(5)	0.702(12)	0.762(8)	0.697(5)	0.763(6)
full range	0.782(1)	0.799(1)	0.611(2)	0.638(2)	0.617(1)	0.646(1)

Table: Average rapidity gap survival factor related to remnant fragmentation for *single dissociative* and *double dissociative* contributions for different ranges of M_{WW} . All uncertainties are statistical only.

Gap survival for double dissociation

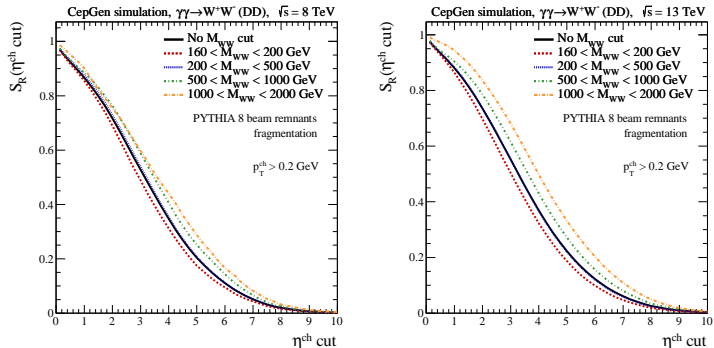


Figure: Gap survival factor for double dissociation as a function of the size of the pseudorapidity veto applied on charged particles emitted from proton remnants, for the diboson mass bins defined in the text and in the figures for $\sqrt{s} = 8$ (left) and 13 (right).

We predict a strong dependence on η_{cut} .

It would be valuable to perform experimental measurements with different η_{cut} .

Gap survival for single dissociation

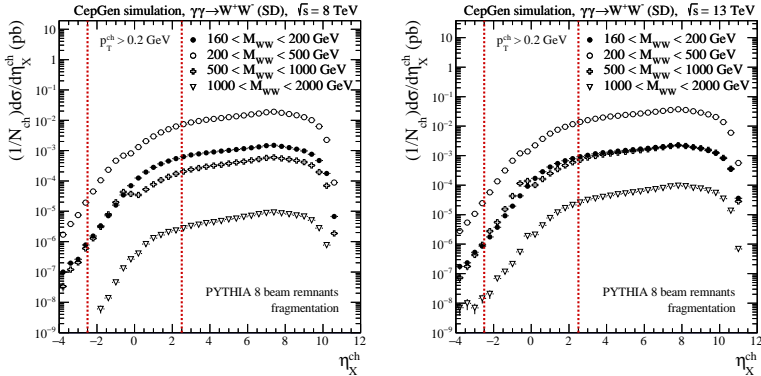


Figure: η_{ch} distribution for single dissociative process for four different windows of M_{WW} : $(2M_W, 200)$, $(200, 500)$, $(500, 1000)$, $(1000, 2000)$, and for $\sqrt{s} = 8$ (left) and 13 (right). The lines show pseudorapidity coverage of ATLAS or CMS detector.

Factorization

$$S_{R,DD} \approx (S_{R,SD})^2 . \quad (16)$$

Such an effect is naively expected when the two fragmentations are independent, which is the case by the model construction.
soft processes will violate the factorisation discussed

Gap survival

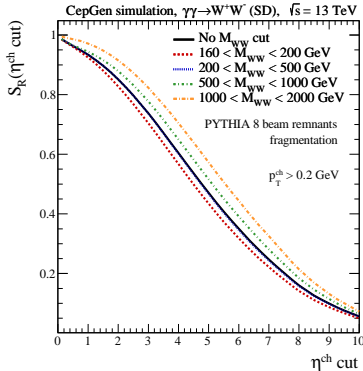
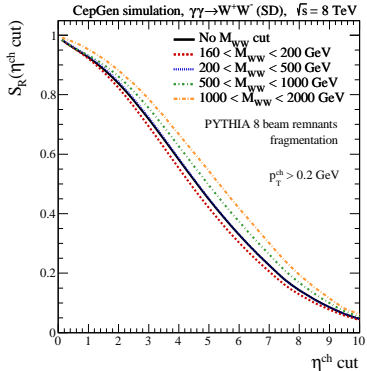


Figure: Gap survival factor for single dissociation as a function of the size of the pseudorapidity veto applied on charged particles emitted from proton remnants, for the diboson mass bins defined in the text and in the figures for $\sqrt{s} = 8$ (left) and 13 (right).

Gap survival

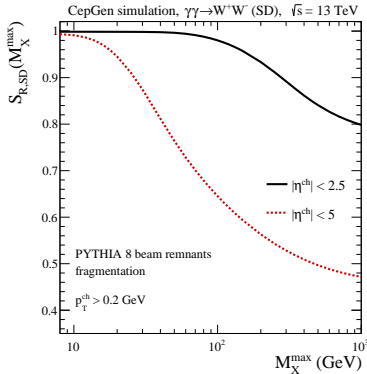
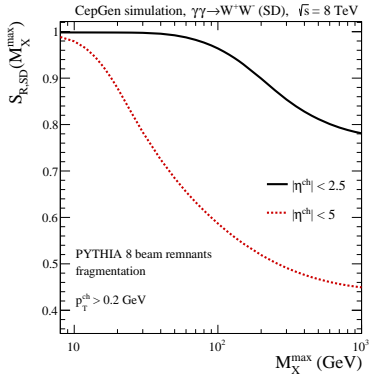


Figure: Rapidity gap survival factor for $|\eta^{ch}| < 2.5$ and $|\eta^{ch}| < 5$ as a function of the upper limit set on M_X , the remnant system invariant mass, for single dissociation.

A comment on the role of soft effects

So far we have not included the **soft** gap survival factors. They are relatively easy to calculate only for double elastic (DE) contribution ([Lebiedowicz, Szczerba](#)). For the “soft” gap survival factors we expect:

$$S_{\text{soft}}(\text{DD}) < S_{\text{soft}}(\text{SD}) < S_{\text{soft}}(\text{DE}) . \quad (17)$$

Some estimates of phase space averaged values were presented ([Harland-Lang, Khoze, Ryskin](#)). A precise kinematics-dependent calculation of soft gap survival factor requires further studies. We expect that the soft gap survival factors may violate the relation $S_R(\text{DD}) = (S_R(\text{SD}))^2$ for the combined (remnant+soft) rapidity gap survival factors.

$pp \rightarrow t\bar{t}$ processes via $\gamma\gamma$ fusion

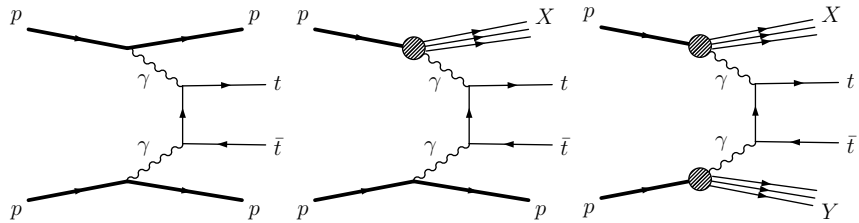


Figure: Classes of processes discussed included. From left to right: elastic-elastic, inelastic-elastic (or equivalently, elastic-inelastic), and inelastic-inelastic contributions.

Total cross sections

Contribution	No cuts	y_{jet} cut
elastic-elastic	0.292	0.292
elastic-inelastic	2*0.544	2*0.439
inelastic-elastic		
inelastic-inelastic	0.983	0.622
all contributions	2.36	1.79

Table: Cross section in fb at $\sqrt{s} = 13$ TeV for different components (left column) and the same when the extra condition on the outgoing jet $|y_{\text{jet}}| > 2.5$ is imposed.

Distributions

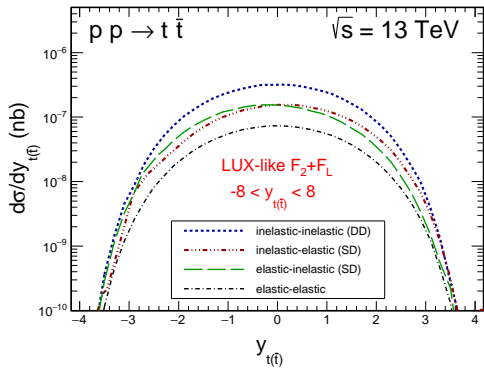


Figure: Rapidity distribution of t or \bar{t} for different components defined in the figure.

Distributions

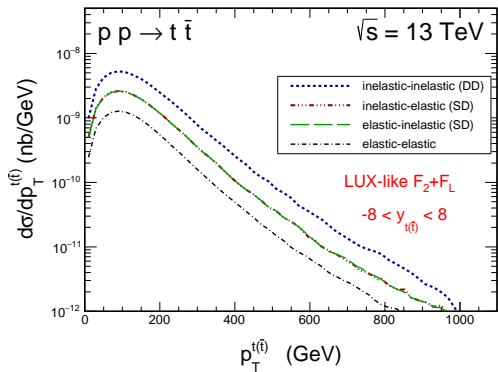


Figure: Transverse momentum distribution of t or \bar{t} for different components defined in the figure.

Applying jet veto

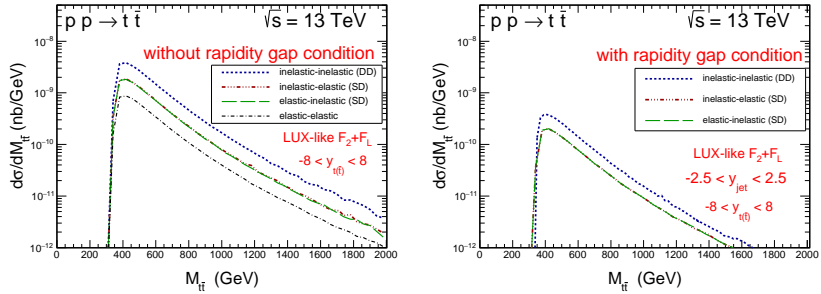


Figure: $t\bar{t}$ invariant mass distribution for different components defined in the figure. The left panel is without imposing the condition on the struck quark/antiquark and the right panel includes the condition.

Further distributions

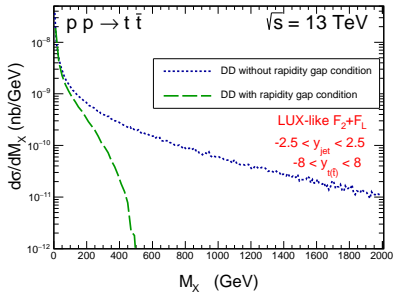
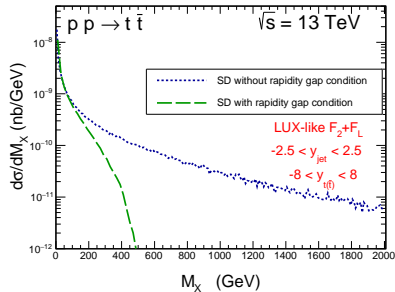


Figure: Distribution in the mass of the dissociated system for single dissociation (left) and double dissociation (right). We show result without and with the rapidity gap condition.

Photon virtualities

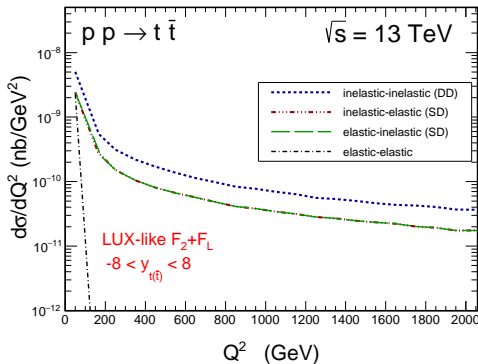


Figure: Photon virtuality distribution for different components defined in the figure.

Photon virtualities

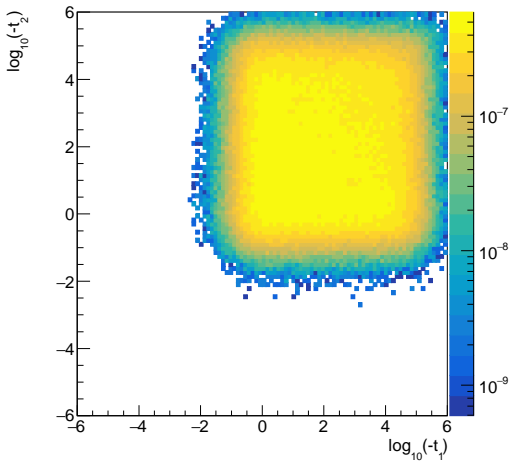


Figure: The two-dimensional $\frac{d^2\sigma}{d\log_{10}(-t_1)d\log_{10}(-t_2)}$ distribution as a function of $\log_{10}(-t_1), \log_{10}(-t_2)$ in nb for the inelastic-inelastic contribution. Here $Q_i^2 = -t_i \cdot 1 \text{ GeV}^2$.

Invariant masses

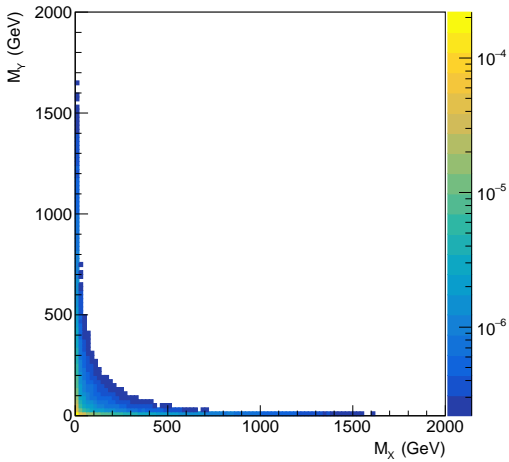


Figure: The two-dimensional $\frac{d^2\sigma}{dM_X dM_Y}$ distribution as a function of $M_X \times M_Y$ in nb/GeV² for the inelastic-inelastic contribution.

Vertex factorization

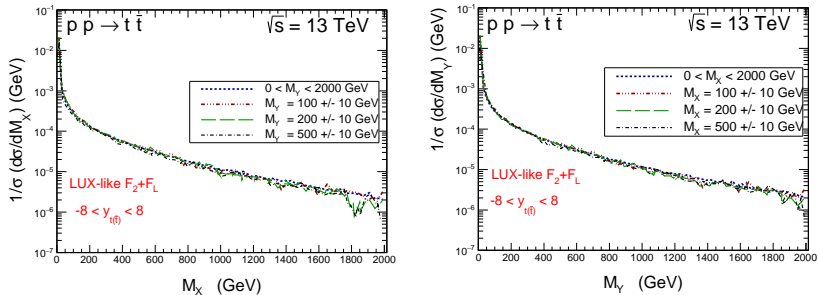


Figure: Distribution in M_X for different windows of M_Y (left) and as a function of M_Y for different windows of M_X (right)

$$\frac{d\sigma(M_X, M_Y)}{dM_X dM_Y} = Cf(M_X)f(M_Y). \quad (18)$$

Consequences of photon transverse momenta

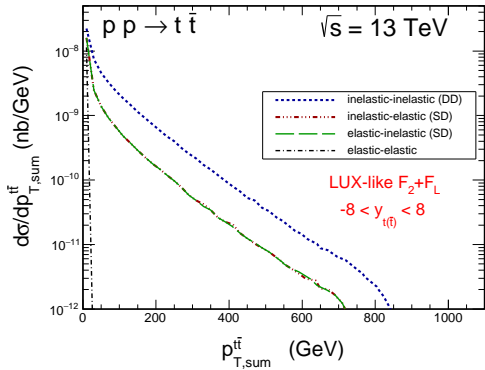


Figure: Distribution in transverse momentum of the t and \bar{t} pairs for elastic - elastic, inelastic-elastic (elastic-inelastic) and inelastic-inelastic contributions for LUX-like structure function.

Gap survival factor

$$S_R(\eta_{\text{cut}}) = 1 - \frac{1}{\sigma} \int_{-\eta_{\text{cut}}}^{\eta_{\text{cut}}} \frac{d\sigma}{d\eta_{\text{jet}}} d\eta_{\text{jet}}, \quad (19)$$

Gap survival factor

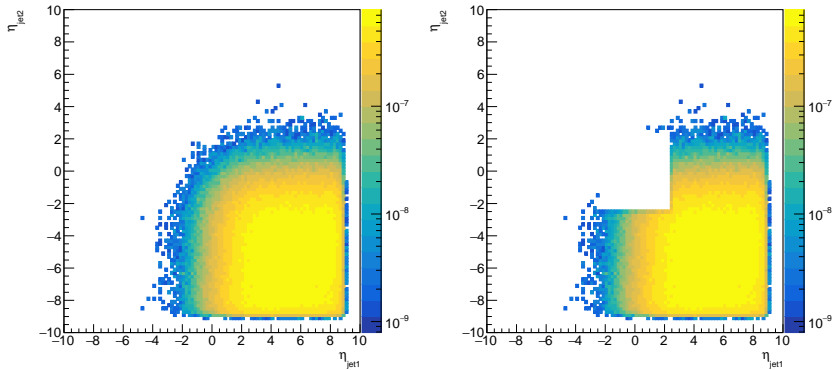


Figure: The two-dimensional $\frac{d^2\sigma}{d\eta_{\text{jet}1} d\eta_{\text{jet}2}}$ distribution as a function of $\eta_{\text{jet}1}$, $\eta_{\text{jet}2}$ in nb. The left panel shows distribution without cuts and the right panel with cuts on $\eta_{\text{jet}1}$ and $\eta_{\text{jet}2}$.

Gap survival factor

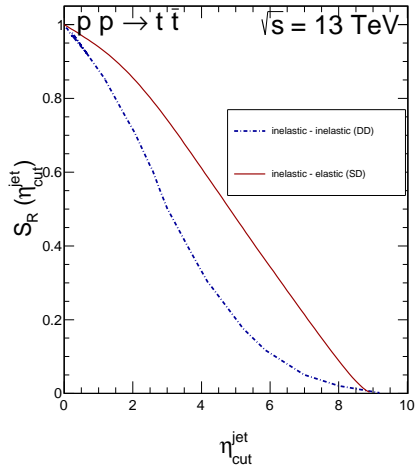


Figure: Gap survival factor for single and double dissociation as a function of the size of the pseudorapidity veto applied on the recoiling jet emitted from proton remnants.

Conclusions on $W^+ W^-$

- ▶ The matrix elements derived by **Nachtmann et al.** have been used.
- ▶ We have obtained cross section of about **1 pb** for the LHC energies. This is about **2 %** of the total integrated cross section dominated by the quark-antiquark annihilation and gluon-gluon fusion.
- ▶ Different combinations of the final states (**elastic-elastic**, **elastic-inelastic**, **inelastic-elastic**, **inelastic-inelastic**) have been considered.
- ▶ The **unintegrated photon fluxes** were calculated based on modern parametrizations of the proton structure functions from the literature.
- ▶ Several differential distributions in W boson transverse momentum and rapidity, WW invariant mass, transverse momentum of the WW pair, mass of the remnant system have been presented.
- ▶ Several correlation observables have been studied. Large contributions from the regions of **large photon virtualities Q^2**

Conclusions. $W^+ W^-$

- ▶ We have presented a decomposition of the cross section into different polarizations of both W bosons. It has been shown that the W (transversally polarized) contribution dominates and constitutes a little bit more than 80 % of the total cross section.
- ▶ The LL (both W longitudinally polarized) contribution is interesting in the context of studying WW interactions or searches beyond the Standard Model.
- ▶ We have quantified the effect of inclusion of longitudinal structure function into the transverse momentum dependent fluxes of photons. A rather small, approximately M_{WW} - independent, effect was found.
- ▶ The discussed here $\gamma\gamma \rightarrow W^+ W^-$ mechanism leads to rather large rapidity separations of W^+ and W^- boson

Conclusions on gap survival factor

- ▶ We have discussed the quantity called “remnant gap survival factor” for the $pp \rightarrow W^+ W^-$ reaction initiated via photon-photon fusion.
- ▶ We have calculated the gap survival factor for single dissociative process **on the parton level**. In such an approach the outgoing parton (jet/mini-jet) is responsible for destroying the rapidity gap. We have discussed the role of valence and sea contributions.
- ▶ We have found that the **hadronisation** only mildly modifies the gap survival factor calculated on the parton level. This may justify approximate treatment of hadronisation of remnants.
- ▶ We have found different values for double and single dissociative processes.

In general, $S_{R,DD} < S_{R,SD}$ and $S_{R,DD} \approx (S_{R,SD})^2$.

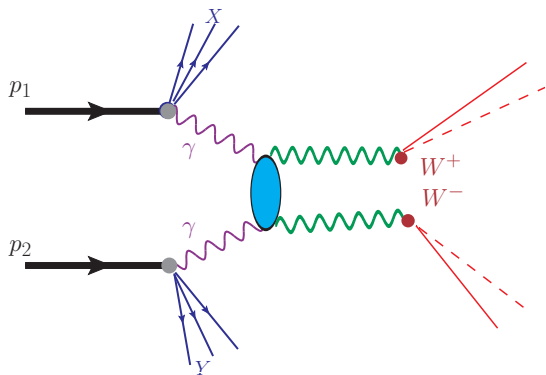
- ▶ We expect that the factorisation observed here for the remnant dissociation and hadronisation will be violated when the soft processes are explicitly included.
- ▶ The larger η_{cut} (upper limit on charged particles pseudorapidity), the smaller rapidity gap survival factor S_R . This holds both for

Conclusions, $t\bar{t}$

- ▶ We have calculated cross sections for $t\bar{t}$ production via $\gamma\gamma$ mechanism in $p p$ collisions **including photon transverse momenta** and using modern parametrizations of proton structure functions.
- ▶ The contribution to the inclusive $t\bar{t}$ is only about 2.5 fb.
$$\sigma_{t\bar{t}}^{ela-ela} < \sigma_{t\bar{t}}^{SD} < \sigma_{t\bar{t}}^{DD}.$$
- ▶ We have calculated **several differential distributions**. Some of them are not accessible in standard EPA.
- ▶ We have shown that large photon virtualities come into the game.
In EPA one has on-shell photons.
- ▶ Gap survival factor due to **proton remnant dissociation(s)** have been calculated for different intervals of rapidity veto.
In our approach $S_R^{DD} = (S_R^{SD})^2$.
- ▶ The gap destroying effects **reverse order of contributions**.
(this should be observed in experiments with rapidity gaps).

Future studies

So far we have calculated $\gamma\gamma \rightarrow W^+W^-$ **inclusive** cross section.
This is not what is done in dedicated studies.



ATLAS and CMS measure leptons and check rapidity gaps.

Include decays of W bosons:

$$W^+ \rightarrow \mu^+, W^- \rightarrow e^- \text{ or}$$

$$W^+ \rightarrow e^+, W^- \rightarrow \mu^-$$